International Journal of Scientific Research in Science, Engineering and Technology
Print ISSN: 2395-1990 | Online ISSN : 2394-4099 (www.ijsrset.com)
doi : https://doi.org/10.32628/IJSRSET21862

Hydrogeological Modelling of Olkaria Domes Geothermal Field to Predict Ground Subsidence

Solomon Kahiga*[1], Nicholas Mariita[2], Njenga Mburu[3]

*[1]Geothermal Energy Training and Research Institute, Dedan Kimathi University of Technology, Nyeri, Kenya
[2]School of Engineering, Dedan Kimathi University of Technology, Nyeri, Kenya
[3]Civil Engineering Department, Dedan Kimathi University of Technology, Nyeri, Kenya

Article Info
Volume 8, Issue 6
Page Number : 25-38

Publication Issue :
November-December-2021

Article History
Accepted : 05 Nov 2021
Published: 14 Nov 2021

ABSTRACT

Ground subsidence studies have been done on Olkaria geothermal field conventionally by comparing levels on benchmarks over years. Interferometric synthetic aperture radar (InSAR) systems have also been used to map surface deformation of small spatial extent. For the prediction of future dynamics of land subsidence in Olkaria due to geothermal resource exploitation, a hydrogeological conceptual model has been developed. In this model, hydrologic geothermal fluid properties are analysed and a relationship between the reservoir and geology of the wells established, subsidence is computed numerically. The model takes into account the hydrogeological condition of Olkaria geothermal field. Hydrological reservoir parameters are computed from well testing data. The study considers the Injectivity indices of the various wells under study as pre-computational indicator of the expected subsidence extents. Both two- and three-dimensional geological cross-sections are modelled with the rockworks software by inputting stratigraphic data for Olkaria domes. Geological simulations are used to study subsidence by assigning the ground formation with virtual material that deformed according to some essential relations in Rockworks computer software. Production zones are determined by a comparison between the well properties and corresponding well geology. Subsidence is then computed by the Tezarghi's modified equation. Cumulative subsidence figures from the computation are in the range of 0.095-0.537m, without any reinjection. Computed values are then mapped in ArcGIS to develop a representative subsidence map. By application of these modelling and numerical computation methods, ground subsidence was effectively predicted using the five selected wells in Olkaria domes field. The hydrogeological model developed, and mapping is an important tool in the planning and development of a reinjection schedule and in subsidence mitigation. Subsidence prediction also is important in design of infrastructure which will be strong enough to resist the forces caused by subsidence.

Keywords : Geothermal, Subsidence, modelling, Geology and Geothermal reservoir

I. INTRODUCTION

Ground subsidence is the gradual or sudden vertical settling or sinking of the ground surface with little or no horizontal movement on the surface due to withdrawal of matter from the subsurface. In geothermal systems, it occurs when geothermal fluids withdrawal is higher than recharge, during well testing and geothermal exploitation, causing a reduction pressure in the pores of the formation. Subsidence also occurs as a result of existence of compressible geologic/ geotechnical formations being overlain by other formations resulting to overburden pressure. A combination of both can result in high levels of subsidence, where geothermal fluids are withdrawn from highly compressible formations.

Therefore, the major causes of ground subsidence include:

(i) Reduction in pore pressure in a reservoir due to higher rates of fluids withdrawal compared to recharge.
(ii) Presence of highly compressible geologic formations within the reservoir.
(iii) Presence of paths of high permeability between feed zones and other formations, and between the production zones and the ground surface [3]

Ground subsidence has greater chances of occurrence in liquid dominated reservoirs which causes instability of geothermal related infrastructure such as pipelines, drains, and well casings. As a result of subsidence, ponds and cracks on the ground surface are bound to form, also causing instability of buildings around the site.

Cases of extreme subsidence have been witnessed in a number of geothermal fields. An example is subsidence in Wairekei field in New Zealand with a maximum recorded rate of 13 metres per year [4]. In Iceland, Svartsengi and Reykjanes have recorded averages of 10mm/yr and 6mm/yr respectively [1]

Ground subsidence studies have been done previously using precise levelling. Precise levelling surveys that have been carried out in Olkaria field are for a single epoch which makes subsidence determination impossible, which requires levelling survey of more than one epoch [6]

Subsidence directly refers to ground deformation. Having extensive information regarding the spatial extent as well as expected magnitude of predicted deformation helps determine cost effective means of quantifying subsidence. This information makes it possible to to generate numerical models representing the geothermal system and from which prediction of ground subsidence can be made. The prediction can then be used for purposes of monitoring and development of a mitigation plan for the associated effects [6]

There are various analytical methods for prediction of ground subsidence but the finite element method (FEM) has proven to be the most powerful tool of all [5]. The theory of Poroelasticity forms the basis for the simulation and prediction of ground subsidence within a field of interest. Solution of subsidence problem can be approached in two ways, i.e., the uncoupled or the coupled modelling. In the latter case the poroelastic as well as fluid dynamic equations are solved together for the pore pressure and medium displacement unknowns.

On the other hand, for the former approach, after determination of fluid pressure distribution within (and around) a reservoir is independently, by either a flow simulator or in-situ measurements, the subsidence of ground surface is computed by only the poroelastic model [2]

II. METHODS AND MATERIAL

In order to achieve the objectives of this study, secondary data was collected. This chapter explains the process of data acquisition, the kind of data collected and the methods applied in data analysis.

For the purposes of this research, five wells were used OW-901A, 0W-902A, OW-910, OW-911 and OW-

921. Of these wells OW-901A, OW-910 and OW921 were production wells, OW-911 a hot reinjection well and OW-902A, a cold reinjection well.

2.1 Data

For the purposes of developing this hydrogeological conceptual model, the following data was acquired from the field:

(i) Wells GIS information including wells coordinates, elevations and type of well.
(ii) Directional drilling data for all directional wells.
(iii) Wells geological data, majorly; lithology, alteration mineralogy, general rock properties and loss of circulation zones.
(iv) Temperature and pressure conditions in the geothermal system.
(v) Pressure transient data from completion well test.
(vi) Reinjection well test data

2.2 Determining position details and geology of well bores

Olkaria domes well details were obtained from Olkaria GIS records. These included the wells co-ordinates and elevations. GIS Shapefiles data was run using Arch Map to produce an orientation map for directional drilled wells.

Well location data was also input in rockworks software to create reference during geological modelling. Geo-referenced well positions were also produced by the rockworks software.

2.3 2D and 3D geological models

The main objective of 2D and 3D modelling in the process of developing a conceptual model was to create a visualization of the natural geological setting of the area to be modelled. Rockworks apply Inverse distance weighting (IDW) interpolation method to do solid modelling from geological data from geological logs of adjacent wells.

Developing a 3D model follows a step by step process from data input to production of the complete model. For this research the following process was followed:

(i) Data acquisition
(ii) Data preparation and quality control
(iii) Data import into the software
(iv) Creating a surface model
(v) Creating a 3D property model
(vi) Presentation of the 2D and 3D models

Rockworks software records well positions and elevations by absolute co-ordinates of the form (x,y,z). Based on the eastings, northings and well elevations, the software then computes well depths, and downhole geological surveys done for both vertical and non-vertical wells. The software recorded well orientation and azimuth for the non-vertical wells.

For the various wells, Rockworks has tools in the Borehole manager menu responsible for creating 2D and/or 3D logs for individual and/or multiple wells.

Since the co-ordinates of the various wells are known, Log profile diagrams were produced which show vertical geologic set up of each well.

The geology of well bores was obtained from the Olkaria geological records of the various wells. This information was obtained from the wells drilling logs which indicated the geologic formations penetrated by the wellbore and general rock properties.

The wells geological logs were entered into the rockworks and modelling was done.

2.4 Subsurface visualization of geothermal wells using the ROCKWORKS

This was done in stages using the ROCKWORKS software as described below:

2.4.1 *Stratigraphic Diagrams*

2D stratigraphic diagrams were drawn to show the thickness and profile of every geologic formation by linking up the log profiles of adjacent wells. The software then applies interpolation to visualize stratigraphy of the intermediate ground between the

wells. By inter-linking 2D stratigraphic layers, 3D stratigraphic models were developed.

2.4.2 *Lithology Diagrams*

Lithology menu in the Borehole management tab in the software helped interpolate the individual well lithologies by inverse distance weighting into a solid model, and create a conceptualized visual model to produce diagrams such as; vertical profile/ cross-section, fence diagrams, plan view slice, geology map and 3D maps of the various parameters that might be in question.

2.5 Reservoir modelling and analysis

The data for determination of the hydrologic properties included well temperature profiles, pressure profiles, well testing data i.e. well heat up data and step pumping test data.

The geothermal fluid inflow zones from the wells was determined from the temperature profiles analysis.

2.5.1 *Reservoir Data computation*

Temperature and pressure logs were obtained from the reservoir department were used to carry out reservoir properties computation. This included developing downhole temperature profiles which were later compared to the lithological logs to determine feed zones/ compressible zones.

Multi-rate injection data was analysed to determine the injectivity indices for the different wells. The injectivity indices served as an indicator of the relative permeability of the wells in this research. This was later used as a check for the subsidence values resulting from subsidence computation.

Geothermal reservoir modelling helps to make predictions about the behaviour of the geothermal fluid flow system such as:

(i) What the potential impact of geothermal resource exploitation on the natural environment is (Surrounding wells, the overlying geological formations).

(ii) What the impact of geothermal production and reinjection at specified wells will be.

The geothermal resource system is represented in a computer model whereby the geology becomes the hydrogeological parameters such as conductivity and stotativity. Hydrologic parameters that impact the geothermal flow system are known as boundary conditions in a model and include areas of discharge as well as recharge (reinjection).

Once a geothermal reservoir model is developed, it can be used in predicting the response of the hydrogeological system to design changes in future. For example, production wells and/or reinjection wells can be added to the model to simulate their impact on the hydraulic heads and flow before they are ever drilled thus helping in cost saving and mitigation of hydrogeological responses such as subsidence.

2.5.2 *Heat-up temperature data analysis*

Raw temperature heat-up data was analysed by plotting temperature profiles of the five wells selected for this study. The temperature profiles were also analysed alongside the lithologic data in order to determine the geology of the feed zone. This would in turn help determine the depth of feed zones and therefore analyse the overburden formations to the feed zones.

2.5.3 *Multi-rate injection test*

This test analysis was conducted based on the reservoir data obtained from the step pumping test for every well. Multi-rate injection test analysis was used to determine injectivity index of the reservoir, which is an important physical reservoir parameter in this study.

The multi-rate injection rates and corresponding downhole pressure were plotted against time and the pressure at the end of each step was extracted from this plot. The extracted pressure at the end of each step was plotted against the corresponding injection rate. This plot generated a scatter with a trending

positive gradient straight line. The slope of this plot provides the measure of the overall well injectivity index.

2.6 Analyse the subsurface profile and estimation of settlement

The rate of extraction of the geothermal fluids from the wells was extracted from the Olkaria Geothermal records. Analysis was done on volume extracted per year to determine volume changes (assuming no reinjection is done).

The value of volume change was to reflect the maximum level of ground subsidence possible.

The volumes were corrected using the planned re-injection plan by the company on the geothermal field to determine the actual volume changes in the reservoir.

These modified Terzaghi's equation was used to determine the amount of shear force exerted on the rocks above the reservoir, and depending on the bearing capacity of the rocks, actual ground subsidence per year will be determined.

III. RESULTS AND DISCUSSION

3.1 Wells location plots

Wells location plot was done by entering the geographical position coordinated obtained from the Olkaria GIS department into Rockworks software. The output was a georeferenced map of the wells location as shown in Figure 3.1. This was for the purpose of sirface modelling, which was done to define spatial extent of the study area as well as model elevation details of each of the wells of interest.

3.2 Stratigraphic and Lithologic logs

After surface modelling was done, the lithologic solid models were developed. The main aim of solid modelling in this study was to simulate the geologic setup of the area through a subsurface conceptual model.

Olkaria Domes field, being a volcanic hosted geothermal field, the hydrogeological system is highly controlled by permeability of the geological formation which in turn has a direct effect on ground subsidence. Through geological modelling it was possible to identify probable positioning of these faults as well as visualize strata boundaries within the study area.

Geological solid modelling was done in 3 steps. First, stratigraphic data obtained from Olkaria well logs was entered into the Rockworks software and 2D well striplogs were modelled.

Second, 3D strip logs were simulated and visualised by defining wellbores diameter as shown in Figure 1. The strip logs also indicate clearly the formation geology of each well as indicated in the lithology legend.

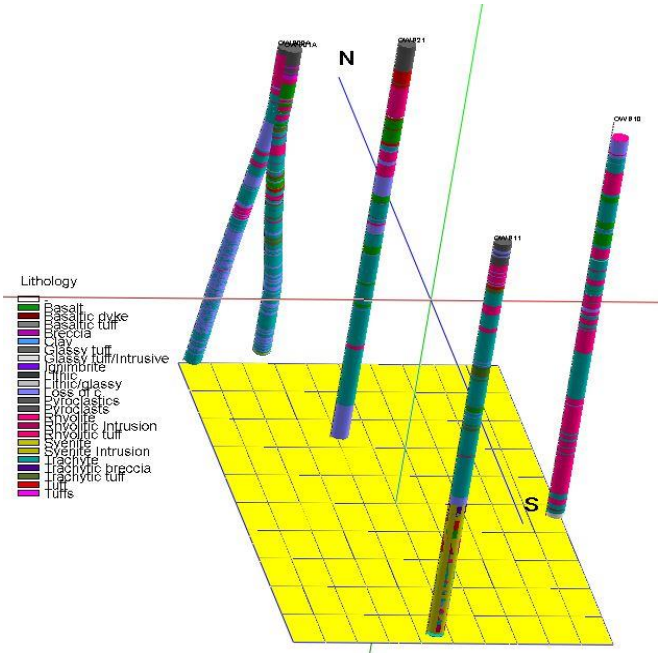

Figure 1: 2D lithologic strip logs

From the 3D strip logs, it is clear that two of the selected five wells for this study were directional wells. The intermediate geologies would later be interpolated from the 3D strip logs to form a 3D solid model as shown in Figure 2.

Lastly, by application of interpolation capabilities of the Rockworks software, a 3D solid block geologic model was developed as indicated in Figure 2.

From this solid model, it is clear that the Geology of the selected part of the Olkaria Domes geothermal field is mainly Trachyte dominated for the better part of the formation and Rhyolite dominated to the Eastern side

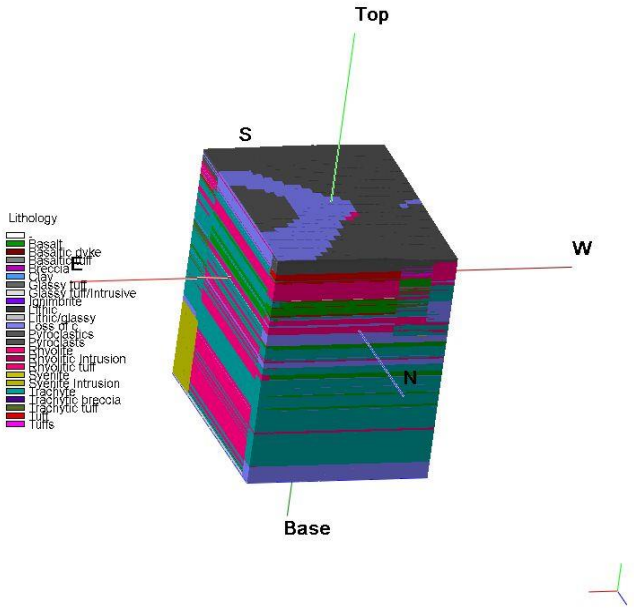

Figure 2: 3D Lithologic solid model

3.3 Reservoir Physics/Reservoir Engineering

Geothermal reservoir physics is a paramount branch in geothermal development at both exploration and utilization stages. There are two major purposes of geothermal reservoir physics. First, is to obtain the nature, reservoir properties and physical condition of a geothermal reservoir system. Second, is to use this information to predict the future response of the reservoir and wells due to exploitation of the resource. The latter can only be achieved through modelling of the reservoir system and subjecting the conceptual model to future exploitation conditions and observing how it behaves.

Well test data acquired from the Olkaria reservoir engineering department was used to do a pre-conceptual modelling analysis in order to determine reservoir properties based on the well completion data provided.

Heat-up temperature profile analysis

The heat-up temperature profiles were plotted for the five wells selected for this study and analysis is done alongside the geologic formations at the various depths. This analysis is done in order to determine the productive/permeable formations so as to help determine the geologic formations overburden to the production formation.

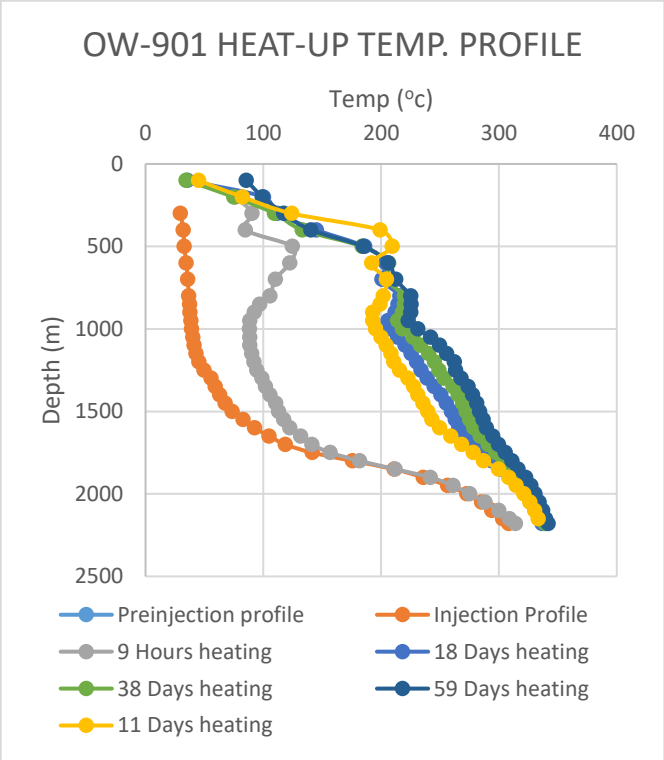

Figure 3: Well OW-901 Temperature profile

From OW-901 temperature profile Figure 3, there is a temperature anomaly at depth 600m and 900m indicating a slight temperature drop from the normal trend. This is an indication that these are cold inflow permeable zones.

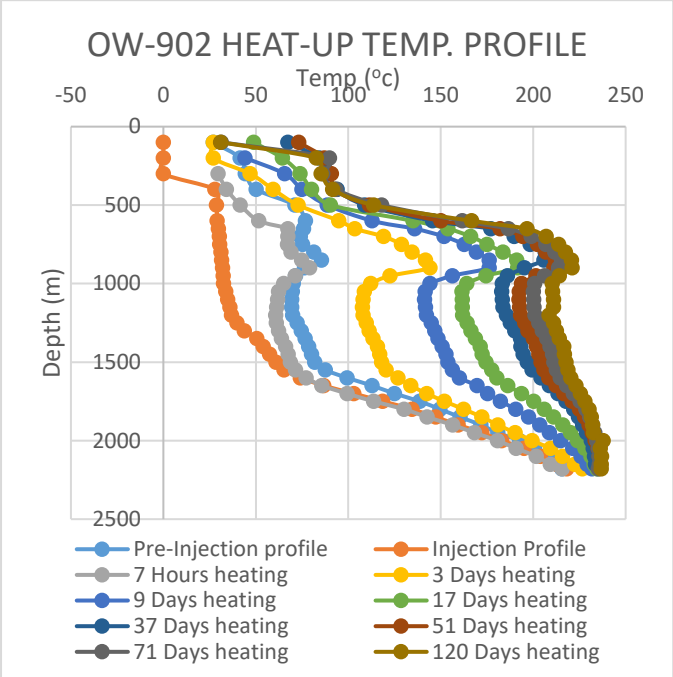

Figure 4: Well OW-902 Temperature profile

From the well OW-902 temperature profile in Figure 4, permeable zones can be identified to be at depths 750m and at 2180m where drastic increase in reservoir temperature is experienced. This shows that these are permeable zones having hot fluid flowing into the well.

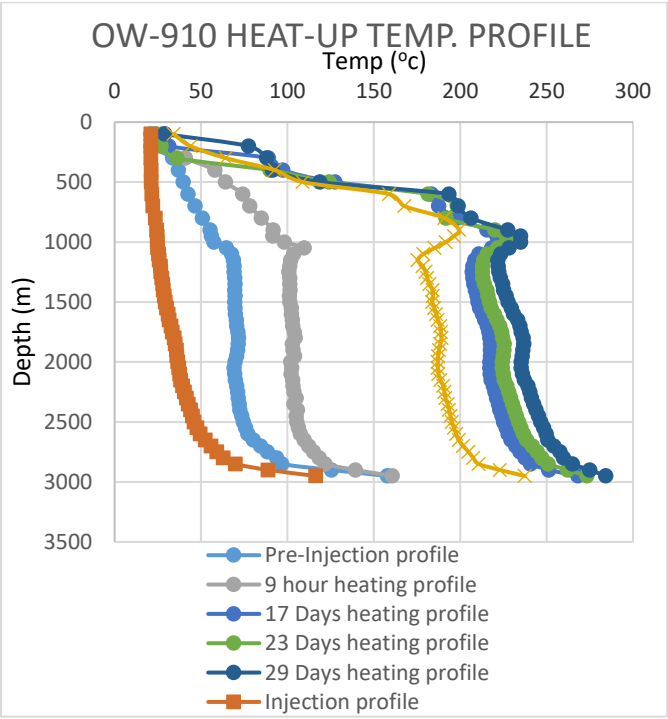

Figure 5: Well OW-910 Temperature profile

The well OW-910 temperature profile in Figure 5 indicated slight temperature increase at depth 600m, and more significant increase at depths 1000m and at 2950m. These zones can be inferred to be permeable zones having hot fluid inflow. Between depth 1150m and 2500m, temperatures remain relatively constant, which can be inferred to be a region experiencing convective mixing of fluids.

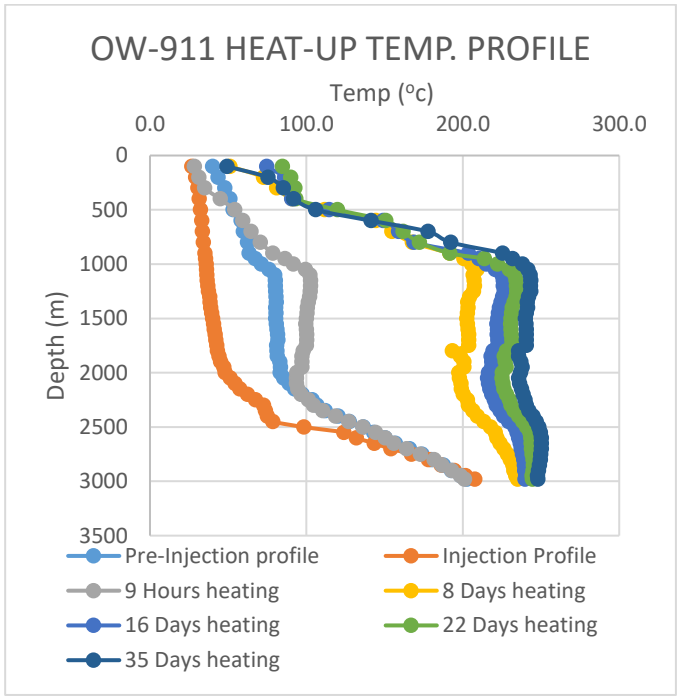

Figure 6 : Well OW-911 Temperature profile

The temperature profile of well OW-911 in Figure 6 indicates gradual temperature increase from depth ground level having a maximum at depth 1000m. The temperature then remains relatively constant with a slight decrease at depth 1800m and a slight increase at depth 2500m. Permeable zones can therefore be inferred to be at depth 1000m, 1800m and 2500m. From depth 1100m to 2400m convective mixing of fluids is probable where the temperatures remain relatively constant.

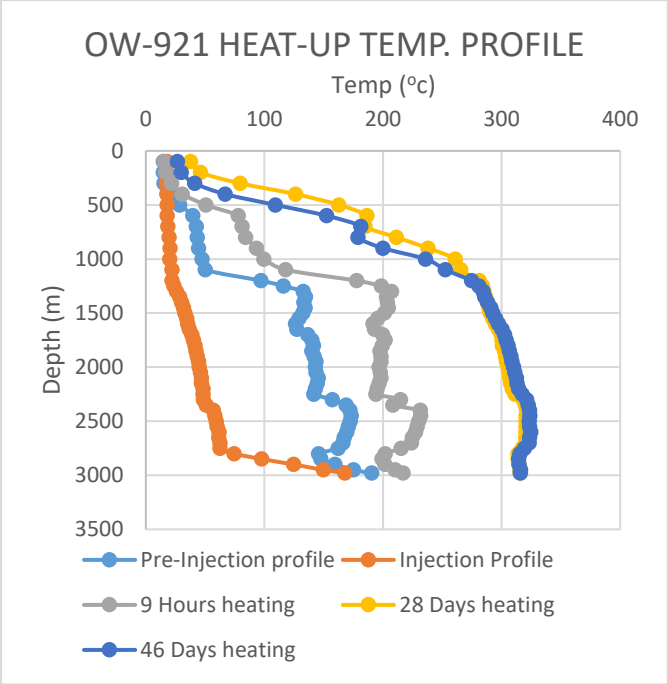

Figure 7 : Well OW-921 Temperature profile

Well OW-921 temperature profile in Figure 7 indicates four permeable zones at depth 1300m, 2400m, 2800m and 3000m. They are hot inflow zones where slight temperature increase is experienced apart from depth 2800m which is a cold inflow zone experiencing a slight decrease in temperature.

3.3.1 Comparison of temperature profiles and geological logs

After comparing the temperature profile logs and the geological data modelled in Rockworks, it was clear that the predicted feed zones as well as zones of high permeability had geological uniformity.

All the predicted feed zones were characterised by Trachytic formations with clayey mineralization. All the predicted zones of high permeability experienced loss of circulation during drilling. In most of the cases where loss of circulation was experienced, it was bordering Trachytic formations.

A conclusion can therefore be drawn that the compressible zones, important in this research are zones of high permeability i.e. experiencing loss of circulation as well as Trachytic formations having clayey mineralization since clay is an expandable mineral.

Multi-rate injection test analysis

This test analysis was done to determine the injectivity index of the various wells. Step pumping data was analysed. Pumping rate and corresponding reservoir pressure were plotted against time as indicated in the upper Figures 8a, 9a and 10a.

Pumping rate was then plotted against pressure at the end of every step and based on the equation: $\boldsymbol{II} = \frac{\Delta \boldsymbol{q}}{\Delta \boldsymbol{p}} = \frac{\Delta \boldsymbol{flow\ rate}}{\Delta \boldsymbol{downhole\ pressure}}$, the Injectivity index was determined from the slope of this plot. This is as indicated in the lower Figures 8b, 9b and 10b.

a)

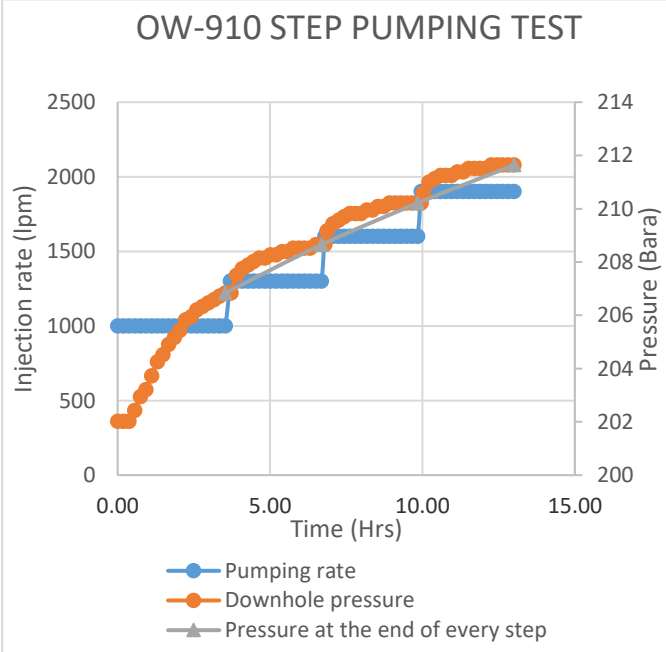

(b)

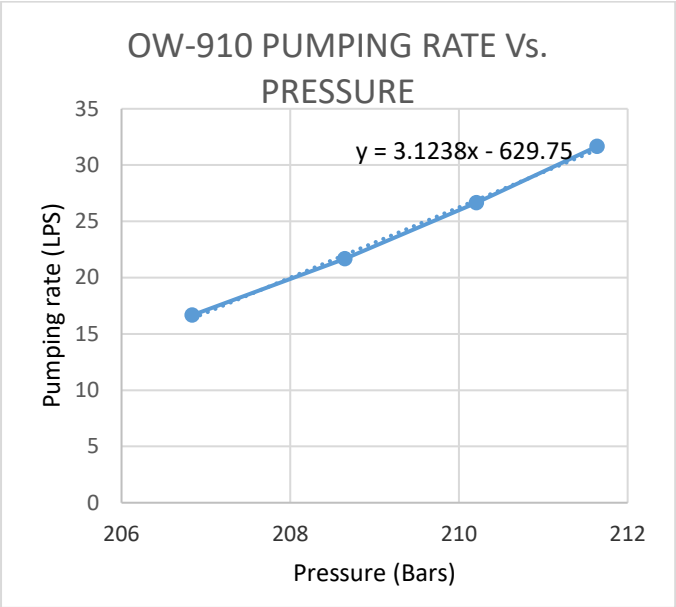

Figure 8 a) : Well OW-910 Step pumping test plot, b): Well OW-910 Injectivity index analysis

Based on this analysis, the Injectivity Index for well OW-910 was 3.12 lps/Bar

a)

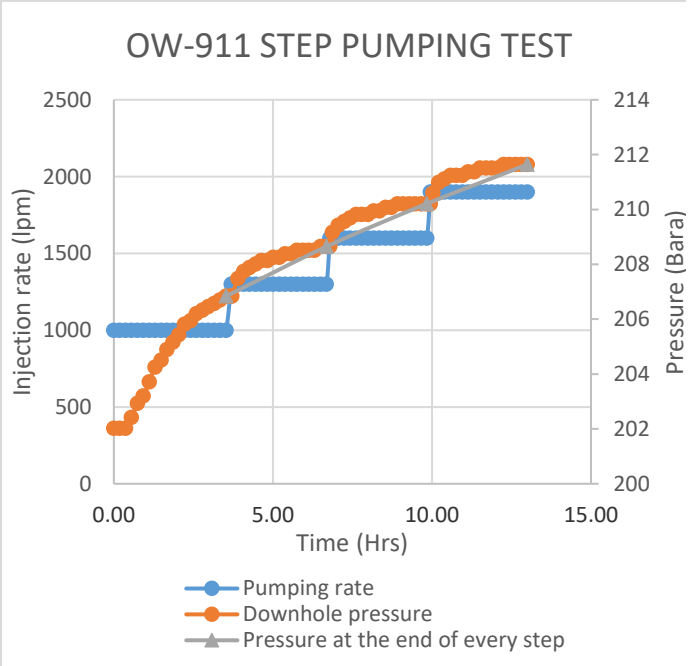

b)

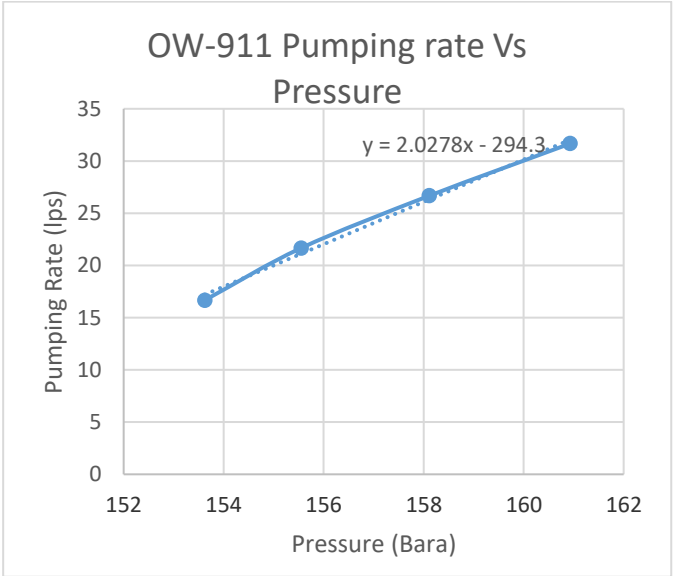

Figure 9a) : Well OW-911 Step pumping test plot, b): Well OW-911 Injectivity index analysis

Based on this analysis, the Injectivity Index for well OW-911 was 2.03 lps/Bar

a)

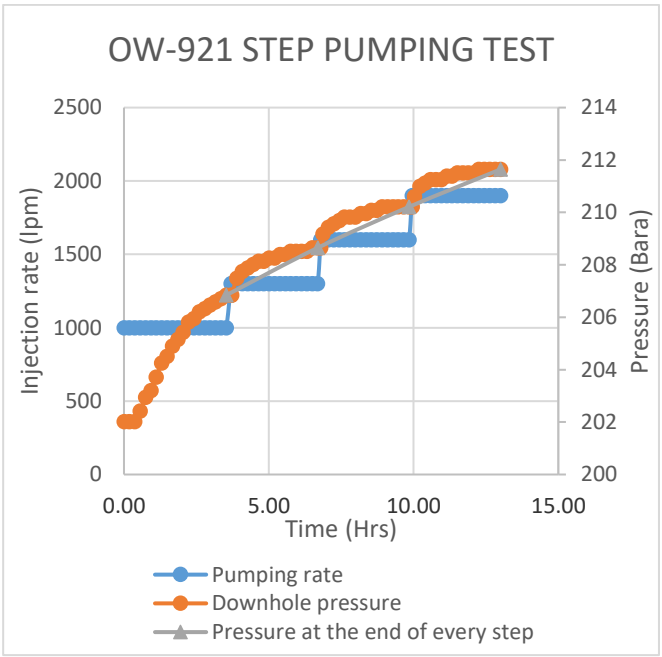

b)

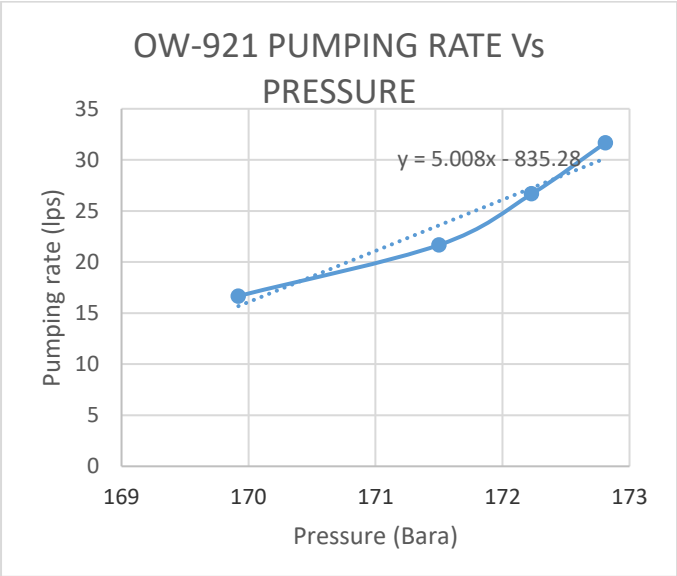

Figure 10 a): Well OW-921 Step pumping test plot, b): Well OW-921 Injectivity index analysis

Based on this analysis, the Injectivity Index for well OW-921 was 5.0 lps/Bar. The injectivity indices were used as a relative indicator of expected subsidence levels.

3.3.2 Relevance of Injectivity Index analysis

Injectivity index, being the ability of a well to accept fluids was an important analysis to carry out to act as a subsidence pre-computation prediction tool. Higher injectivity index value translated to a higher productivity value for production wells. Wells with a high Injectivity index meant that they were more permeable and therefore had larger compressible geological formations.

The injectivity indices from the analysis indicated well OW-921 was the most permeable while well OW-911 was the least permeable.

3.4 Subsidence Analysis

This was the main objective of this research. Ground subsidence was modelled by using both the 3D geological models and the heat flow reservoir model being used as a substitute of mass flow model.

A 2D subsidence prediction map was prepared using the computed subsidence values. Ground subsidence was also computed at well locations by use of the downhole lithological data. By the interpolation capabilities of rockworks, a subsidence prediction map was prepared and the maps from the two methods compared. The resulting settlement values were then compared to the recorded subsidence values from survey of Olkaria field.

3.4.1 Geotechnical properties of stratigraphic layers

To predict ground subsidence due to overburden pressure from formations overlying the feed zone formations, the geotechnical properties of the stratigraphic layers was determined. The formations were divided into three major categories i.e. Pyroclasts, Rhyolites and Trachytes. The geotechnical properties important for this study were unit weight and coefficient of compressibility and were as in Table I.

TABLE I: GEOTECHNICAL PROPERTIES OF ROCK FORMATIONS

Rock Type	Average Sat. Unit Weight (kN/m3)	Coefficient of Compressibility (C')		
		Min	Avg.	Max
Pyroclasts	20 - 22	120	170	600
Trachytes	22 - 25	150	165	700
Rhyolites	24 - 26	220	260	900

3.5 Subsidence computation

Based on the available data for this research, the modified Terzaghi's equation was used in this research.

$$S = \frac{H}{C'} \ln \frac{\sigma' v + \Delta p}{\sigma' v}$$

Where,

S - Subsidence

H – Thickness of compressible layer

C' – Coefficient of compressibility

σ' – Initial vertical effective stress at mid-height of compressible layer

Δp – Increase in vertical effective stress

In order to carry out this computation, 2D interpolated geological logs from Rockworks were used to refer to in order determine the input parameters in the modified Terzaghi's equation.

The thickness of the compressible stratigraphic unit (Assumed to be the production formation) was determined from the depths modelled in Rockworks.

The coefficient of compressibility used was determined from the average values of geotechnical properties relative to the corresponding formation.

Initial vertical stress (σ'_v) was determined from the equation

$$\sigma' v = \sigma - u$$

Where,

σ - Is the total vertical stress at the midpoint of the formation (which is the product of the saturated unit weight of a formation and its thickness) i.e. $\sigma = \gamma 1H1 + \gamma 2H2 + \cdots \ldots \ldots \ldots + \gamma nHn$

u – Pore pressure midpoint of the formation which is a product of unit weight of geothermal fluid and the depth of formation below the first feed zone.

The vertical effective stress, was found to be a term relating to consolidation of the formations. It was determined from the equation:

$\Delta p = \gamma w * Hfeed\ zone$

Where,

γw - Unit weight of the geothermal fluid

$Hfeed\ zone$ – Thickness of the feed zone

An increase in vertical effective stress was found to be attributed to either reduction in pore pressure or an increase in the overburden load.

The subsidence values obtained after computation were as indicated in Table II. Subsidence computation sheet is as indicated in Figure 11.

TABLE II: COMPUTED SUBSIDENCE VALUES

Well no	Northings	Eastings	Elevation	Cumulative Subsidence (m)
OW-901A	9900769	201978.7	1898.92	0.206817281
OW-910	9899738	203733.2	1994.96	0.179897113
OW-921	9900766	202656	1944.41	0.536845081
OW-902	9899013	201682	1951.57	0.104204168
OW-911	9898287	202725.7	1979.52	0.095498406

3.6 Subsidence Mapping

Subsidence was computed for individual wells, meaning that the values were wells point based. In order to develop a representative 2D ground surface subsidence map, interpolation was done in ArcGIS in order to have a representative inter-wells subsidence.

The subsidence map from the computed subsidence values was created in ArcGIS. First, the (x,y) wells co-ordinates data was input in ArcMap to give point locations of the wells. Secondly, Layering was done in order to have the created wells location as a shapefile.

After having georeferenced point locations in ArcMap, each point was assigned the corresponding settlement value. A settlement prediction map was then prepared by converting the created vector points into a raster layer as per the settlement values.

By use of Kriging inverse distance interpolation method, surface subsidence was developed between the reference points i.e. the wells. This produced a subsidence map indicative of the relative subsidence range from the computed individual wells subsidence values as indicated in Figure 12.

In conclusion, maximum subsidence values were recorded around well OW-921 and the least values around well OW-911. This was in line with the prediction from the Injectivity index analysis where

relatively well OW-921 had the highest value and well OW-911 the least.

This also is in line with the fact that well OW-911 was a re-injection well therefore minimum subsidence values would be expected as compared to the rest of the wells which were production wells.

T2 =(D2/E2)*LN((O2+S2)/O2)

	A	B	C	D	E	F	G	H	I	J	K	L	M	N	O	P	Q	R	S	T	U
1	D1	D2	Litho	H (m)	C'	γ(Rock) (KN/m3)	γH (KN/m2)	Cummulative γH (KN/m2)	Vertical Stress at mid height (δ)	Hw (m)	γ(Brine) (KN/m3)	γHw (KN/m2)	Cummulative γHw (KN/m2)	Pore pressure mid height (μ)	Effective stress mid-height	Change in reservoir depth		Load		Settlement (m)	cummulative settlement (m)
2	0	206	Pyroclast	206	170	21	4326	4326	2163	0	10.27	0	0	0	2163	1	3	10.27	13.27	0.007411462	0.005739886
3	206	446	Rhyolite	240	260	25	6000	10326	7326	33.33	10.27	342.2991	342.2991	171.14955	7154.85045	1	3	10.27	13.27	0.001710432	0.007450318
4	446	480	Trachyte	34	165	23	782	11108	10717	33.33	10.27	342.2991	684.5982	513.44865	10203.55135	1	3	10.27	13.27	0.000267813	0.007718131
5	480	524	Rhyolite	44	260	25	1100	12208	11658	33.33	10.27	342.2991	1026.8973	855.74775	10802.25225	1	3	10.27	13.27	0.000207764	0.007925895
6	524	546	Trachyte	22	165	23	506	12714	12461	0	10.27	0	1026.8973	1026.8973	11434.1027	1	3	10.27	13.27	0.000154652	0.008080547
7	546	568	Rhyolite	22	260	25	550	13264	12989	0	10.27	0	1026.8973	1026.8973	11962.1027	1	3	10.27	13.27	9.38149E-05	0.008174362
8	568	624	Trachyte	56	165	23	1288	14552	13908	0	10.27	0	1026.8973	1026.8973	12881.1027	1	3	10.27	13.27	0.000349461	0.008523822
9	624	626	Trachyte	2	165	23	46	14598	14575	0	10.27	0	1026.8973	1026.8973	13548.1027	1	3	10.27	13.27	1.18666E-05	0.008535689
10	626	628	Rhyolite	2	260	25	50	14648	14623	0	10.27	0	1026.8973	1026.8973	13596.1027	1	3	10.27	13.27	7.50415E-06	0.008543193
11	628	654	Trachyte	26	165	23	598	15246	14947	0	10.27	0	1026.8973	1026.8973	13920.1027	1	3	10.27	13.27	0.000150145	0.008693338
12	654	684	Rhyolite	30	260	25	750	15996	15621	0	10.27	0	1026.8973	1026.8973	14594.1027	1	3	10.27	13.27	0.000104868	0.008798206
13	684	746	Trachyte	62	165	23	1426	17422	16709	0	10.27	0	1026.8973	1026.8973	15682.1027	1	3	10.27	13.27	0.000317827	0.009116033
14	746	850	Rhyolite	104	260	25	2600	20022	18722	0	10.27	0	1026.8973	1026.8973	17695.1027	1	3	10.27	13.27	0.000299858	0.009415891
15	850	932	Trachyte	82	165	23	1886	21908	20965	50	10.27	513.5	1540.3973	1283.6473	19681.3527	1	3	10.27	13.27	0.000334965	0.009750856
16	932	932	Trachyte	0	165	23	0	21908	21908	50	10.27	513.5	2053.8973	1797.1473	20110.8527	1	3	10.27	13.27	0	0.009750856
17	932	952	Trachyte	20	165	23	460	22368	22138	50	10.27	513.5	2567.3973	2310.6473	19827.3527	1	3	10.27	13.27	8.10974E-05	0.009831953
18	952	960	Rhyolite	8	260	25	200	22568	22468	50	10.27	513.5	3080.8973	2824.1473	19643.8527	1	3	10.27	13.27	2.07785E-05	0.009852732
19	960	1042	Trachyte	82	165	23	1886	24454	23511	50	10.27	513.5	3594.3973	3337.6473	20173.3527	1	3	10.27	13.27	0.000326798	0.01017953
20	1042	1050	Trachyte	8	165	23	184	24638	24546	0	10.27	0	3594.3973	3594.3973	20951.6027	1	3	10.27	13.27	3.06989E-05	0.010210229
21	1050	1078	Trachyte	28	165	23	644	25282	24960	0	10.27	0	3594.3973	3594.3973	21365.6027	1	3	10.27	13.27	0.000105365	0.010315594
22	1078	1090	Pyroclast	12	170	21	252	25534	25408	0	10.27	0	3594.3973	3594.3973	21813.6027	1	3	10.27	13.27	4.29283E-05	0.010358522
23	1090	1106	Rhyolite	16	260	25	400	25934	25734	0	10.27	0	3594.3973	3594.3973	22139.6027	1	3	10.27	13.27	3.68738E-05	0.010395396
24	1106	1116	Pyroclast	10	170	21	210	26144	26039	0	10.27	0	3594.3973	3594.3973	22444.6027	1	3	10.27	13.27	3.47682E-05	0.010430164
25	1116	1148	Rhyolite	32	260	25	800	26944	26544	0	10.27	0	3594.3973	3594.3973	22949.6027	1	3	10.27	13.27	7.11454E-05	0.010501309
26	1148	1160	Rhyolite	12	260	25	300	27244	27094	0	10.27	0	3594.3973	3594.3973	23499.6027	1	3	10.27	13.27	2.60553E-05	0.010527365

WELL OW-901A | WELL OW-902 | WELL OW-910 | WELL OW-911 | WELL OW-921

Figure 11: Ground subsidence computation sheet

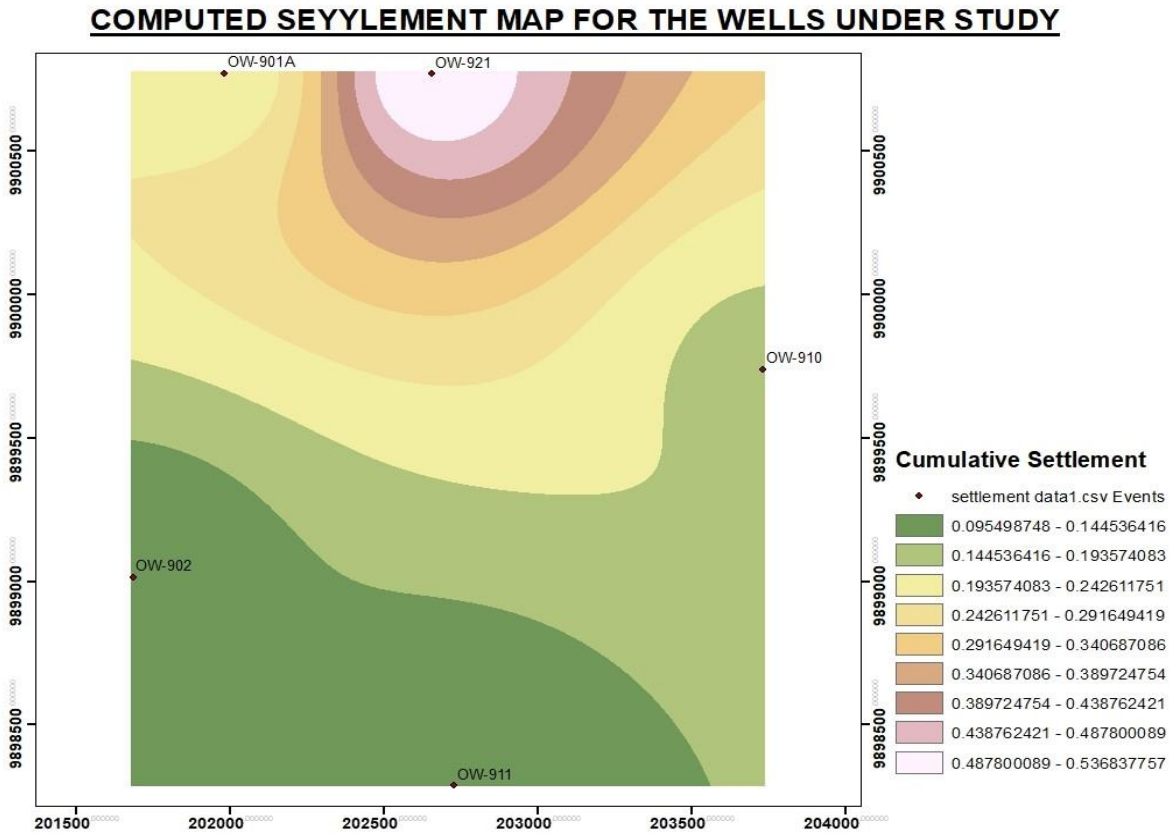

Figure 12: Computed Subsidence map from ArcGIS

3.7 Model validation

Subsidence in Olkaria Domes Geothermal field has not been monitored using precise surveying methods.
The subsidence prediction model was validated by correlating the computed subsidence values from the model and the deformation rate values from InSAR techniques.
Five points were used in this validation, two of which are well points and three intermediate points as indicated in Table 4.3.
Studies show that maximum subsidence occur in the range of 7-12 years [7]. A maximum settlement period of 10 years was adopted for this study. The cumulative subsidence prediction from the Hydrogeological model were corrected to average subsidence per year then compared with the prediction from InSAR technique.

TABLE III: PREDICTED SUBSIDENCE USING INSAR TECHNIQUE VS USING THE HYDROGEOLOGICAL MODEL

S/ No	Validation Point/ Point coordinates	Computed cumulative Subsidence (mm)	Average Computed subsidence (mm/yr)	InSAR Deformation (mm/yr)
1	OW-901A	193.5741	19.35741	14.9
2	OW-910	144.5364	14.45364	14.9
3	(202000, 9897000)	144.5364	14.45364	12.0
4	(202000,99 00000)	193.5741	19.35741	14.9
5	(203500,98 97000)	144.5364	14.45364	14.9

The results of the computed subsidence in this study and the predicted subsidence from InSAR techniques were then plotted to evaluate how they compare as shown in Figure 13.

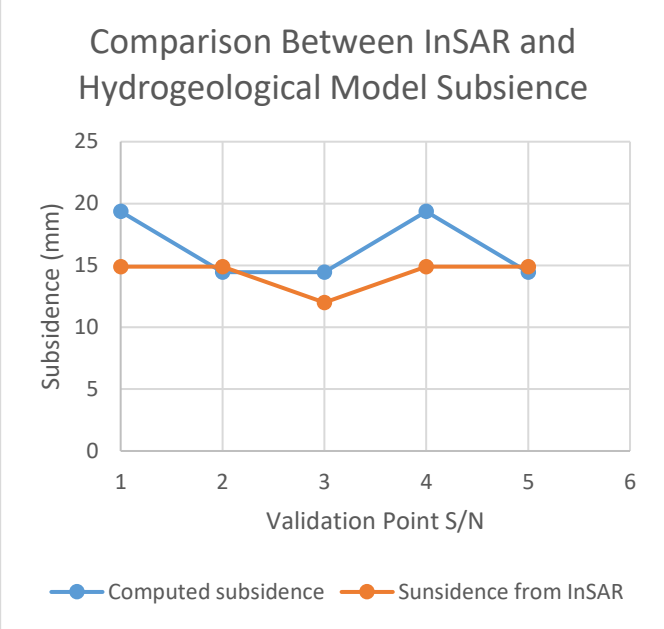

Figure 13: Predicted subsidence using InSAR technique and from the Hydrogeological model plots

The subsidence prediction from InSAR techniques and that from the Hydrogeological model were found to fairly compare. Therefore in conclusion, the model was found to be reliable in subsidence prediction for both new geothermal fields under exploration and Geothermal fields under exploitation.

IV. CONCLUSION

Through 3D stratigraphic modelling, a realistic subsurface conceptual model were developed. Based on the inverse distance interpolation capabilities of Rockworks software, complex geological features specific to the study area were modelled. Through geologic simulation also, key input data to subsidence computation was obtained. By the above capabilities of Rockworks software, a realistic geological conceptual model was developed and visualized as well.
Through reservoir data analysis, important correlation between the wells temperature profile and the lithological formations was developed. Anomalies in the downhole temperature profile were used to

determine feed zones. It is through the determination of feed zones that a trend was established linking trachytic formations with clayey mineralogy as major feed zones. These zones were considered to be the compressible formations. By geological positioning of the compressible formations, the geotechnical properties of the overlaying formations, and the hydraulic properties of geothermal fluid in the feed zones, subsidence was computed.

The computed subsidence was mapped in ArcGIS to develop a computed subsidence map. This was done through Kriging interpolation method to determine inter-wells subsidence values. The interpolated subsidence values were used in rasterization and mapping of the wells location to develop a conceptual subsidence map.

The Hydrogeological model was validated using predicted subsidence values from InSAR techniques and the values fell within range. This conceptual model coupled with numerical computations and analysis therefore resulted to a reliable hydrogeological model. This proved that the model under study could be used for prediction of subsidence in relatively new geothermal fields and fields under exploitation in any geothermal field from as early as the geothermal exploration stage.

V. REFERENCES

[1]. Eysteinsson. (2000). Elevation and gravity changes at geothermal fields on the Reykjanes peninsula,. Proceedings of World Geothermal Congress 2000 Kyushu - Tohoku, Japan.

[2]. Giuseppe et al. (2001). Finite element analysis of land subsidence. International Journal For Numerical And Analytical Methods In Geomechanics, Vol 25, pp307-327.

[3]. Jennifer, A. O. (2010). Environmental and Social Considerations in Geothermal Development. Sydney, Australia: FIG Congress.

[4]. KAPA systems. (2000). Positive social and environmental impacts from the use of geothermal energy. in: Overview of European geothermal industry and technology.Athens, Greece & EGEC. Geothermie, webpage http://www.geothermie.de/egec-geothernet/positive_social_and_environmenta.htm.

[5]. Najjar and Zaman. (1993). Numerical modelling of ground subsidence due to mining. Rock mech. mining Sci. & Geomech, Vol 30, pp1445-1448.

[6]. Wesley and Fitriani. (2016). Subsidence surveys at Olkaria geothermal field, Kenya. Journal of Spatial Science, Vol 62, pp195-205.

[7]. Cui, X. (2020). Calculation of Residual Surface Subsidence Above Abandoned Longwall Coal Mining. Sustainability, 12(4), 1528

Cite this article as :

Solomon Kahiga, Nicholas Mariita, Njenga Mburu, "Hydrogeological modelling of Olkaria domes geothermal field to predict ground subsidence", International Journal of Scientific Research in Science, Engineering and Technology (IJSRSET), Online ISSN : 2394-4099, Print ISSN : 2395-1990, Volume 8 Issue 6, pp. 25-38, November-December 2021. Available at doi : https://doi.org/10.32628/IJSRSET21862
Journal URL : https://ijsrset.com/IJSRSET21862